JETIR.ORG ISSN: 2349-5162 | ESTD Year : 2014 | Monthly Issue
JOURNAL OF EMERGING TECHNOLOGIES AND INNOVATIVE RESEARCH (JETIR)
An International Scholarly Open Access, Peer-reviewed, Refereed Journal

Structural and Optical Properties of $Sm_xCu_{(1-x)}Fe_2O_4$ Nano-Ferrite

Sanjay Ramteke[1*]

[1*] Associate Professor , Department of physics, S. P. Mahavidyalaya, Chandrapur,(M.S.), India

*Corresponding Author: Email:- sanjuram1608@gmail.com

Abstract:

In this work, $Sm_xCu_{(1-x)}Fe_2O_4$ (x = 0.02 to 0.10) compound synthesized using microwave assisted sol-gel technique. The synthesized series of compound were studied by using X-ray diffraction Spectrometer, Fourier-Transform Infra-Red Spectroscopy and Ultra Violet- Visible spectroscopic characterization. The structural analytic behaviour confirmed the formation of tetragonal crystals structure and high purity of the compound. The analysis confirmed that the formation of tetragonal unit cell structure with (211) is the highly dominating orientation. The surface analysis confirmed presence of metal oxide tetragonal and octahedral ions along with -OH and nitrite residuals. The Ultra Violet- Visible spectral analysis showed that the band-gap values can be estimated

Keywords: Inorganic semiconductor, FTIR, $CuFe_2O_4$, XRD, band-gap

I. Introduction

The materials are designed to fulfil requirements of the specific area of science and technology. Metal ferrous oxides received prominent attention due to their spinal structure, high thermodynamic stability, good electrical conductivity, and corrosion resistance nature. These materials have applied applications in field of microwave devices, magnets, computer manufactures industries etc. [1-4]. $CuFe_2O_4$ have studied extensively for the mentioned applications due to its spinal structure and good thermal as well as electrical stability [5]. Further, $CuFe_2O_4$ material and doped $CuFe_2O_4$ materials have extensively used for making sensors, magnetic and optical devices, memory and spintronic devices etc [6,7]. The band optical band of the compound is suitable for catalytic activities, color mapping, and other applications.

The impurities of the transition and rare-earth metal ions restructured the band structure making quasi-stable energies. These doping helps to improve optoelectronic properties of $CuFe_2O_4$ material. In last decades, several elements like Ce, Zn, Ag, Sr, Ho, Ru, In and Zr were doped with $CuFe_2O_4$ material and used for various applied applications [8-13]. The dopant ions change metal ion distribution in the lattice structure modifying crystal structure, electrical, optical, magnetic properties [8,14-16]. Rare-earth metal ions have inherent optical, electrical and magnetic properties due to strong spin-orbit coupling. The rare-earth metal ions along with $CuFe_2O_4$ arise 3d-4f coupling between the host and rare-earth metal ions which alters the properties of $CuFe_2O_4$ compounds.

These materials can be synthesized using ceramic method, combustion method, precipitation method, and solid-state reaction method [13,17-20]. In this research paper, $Sm_xCu_{(1-x)}Fe_2O_4$ (x=0.02 to 0.10) material samples were prepared using microwave assisted sol-gel technique. The micro-structural and structural properties of the synthesized material samples were carried out by X-ray diffraction spectroscopy (XRD). Also, the optical properties are studied by using Fourier-Transform Infra-Red (FTIR) and Ultra Violet-Visible (UV-Vis) spectroscopic measurements.

II. **Experimental**

Material Synthesis

$Sm_xCu_{(1-x)}Fe_2O_4$ (x=0.02 to 0.10) material samples were prepared by microwave assisted sol-gel method. The starting reagents for the sample preparation were Samarium Nitrate [Sm(NO□)□], Copper Nitrate [$Cu(NO_3)_2$], Ferric nitrate [Fe(NO□)□(H□O)□], and urea. In beginning, the stoichiometric amounts of all the starting reagents were dissolved in double distilled water and mix together. The mixture was stirred for 10 min at 30 °C by using magnetic stirrer. Later, the mixture heated for 3 hrs in a microwave until the solution burnt and turned to foamy brown ash. The product left for some time to reach room temperature, and crushed for 4 hrs using mortar and pastel. Later, crystalline powder was annealed at 750 °C for 7 hrs in muffle furnace. The obtained compound left to reach room temperature and the powder crushed for 4 hrs. The obtained samples kept in tubes to avoid from moisture. The prepared sample series sent for XRD, FTIR, and UV-Vis spectroscopy.

III. Results and Discussion

3.1 Structural Analysis

The structural analysis of $Sm_xCu_{(1-x)}Fe_2O_4$ compound is carried out by using XRD patterns, as shown in Fig. (1). The X-ray diffraction (XRD) patterns were measured between 20° to 80°. The measured XRD data were well matched with standard XRD PDF card number 9011012 (dotted lines in the figure). This suggests the synthesized samples has tetragonal crystal phase with a = 5.8 Å and

c = 8.73 Å; also the expected volume of a synthesized comound's unit cell is 293.677 Å^3. The space group of the synthesized samples was *I4$_1$/amd*. The observed peak positions with reflection plane values are 29.87° (112), 34.45° (103), 36.04° (211), 37.19° (202), 44.17° (220), 47° (213), 57.16° (303), 58.28° (321), 62.28° (224), and 64° (400). The most intense peak position with reflection plane values for all Sm concentrations is 36.04° (211). The peak intensity decreased with increasing Sm ion concentration in $CuFe_2O_4$. The standard peak positions are matched with the experimental data which confirmed the synthesized Sm doped $CuFe_2O_4$ compounds was in single phase.

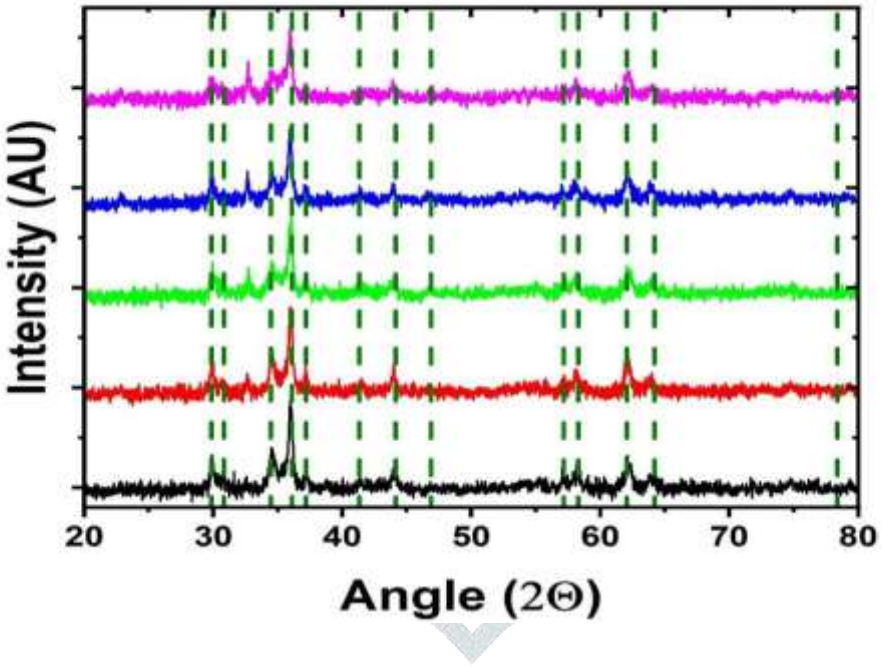

Figure(1). XRD data for $Sm_xCu_{(1-x)}Fe_2O_4$ (x=0.02 to 0.10) compound

3.2 FTIR Analysis

This analysis helps to understand functional groups present at compound's surface. Fig. 2 shows FTIR spectra for $Sm_xCu_{(1-x)}Fe_2O_4$ compounds measured in a range of 4000 – 400 cm^{-1}. The figures shows the multiple absorption peaks in a region of 3500 – 1500 cm^{-1} due to stretching vibration of –OH group which are due to the leftover water molecules present during the producing process[21]. However, absorption bands near 1500 cm^{-1} were prominently due to the availability of nitrate group residual from the preparation process of the samples [22]. The absorption peaks closer to in a range of 470 – 480 cm-1 were due to stretching vibrations of octahedral complexes due to ferrite metal ions [23]. On the other hand, peak in range of 680 – 700 cm-1 were due to the tetrahedral site of Cu^{2+} - O^{2-} metal oxide ions [23].

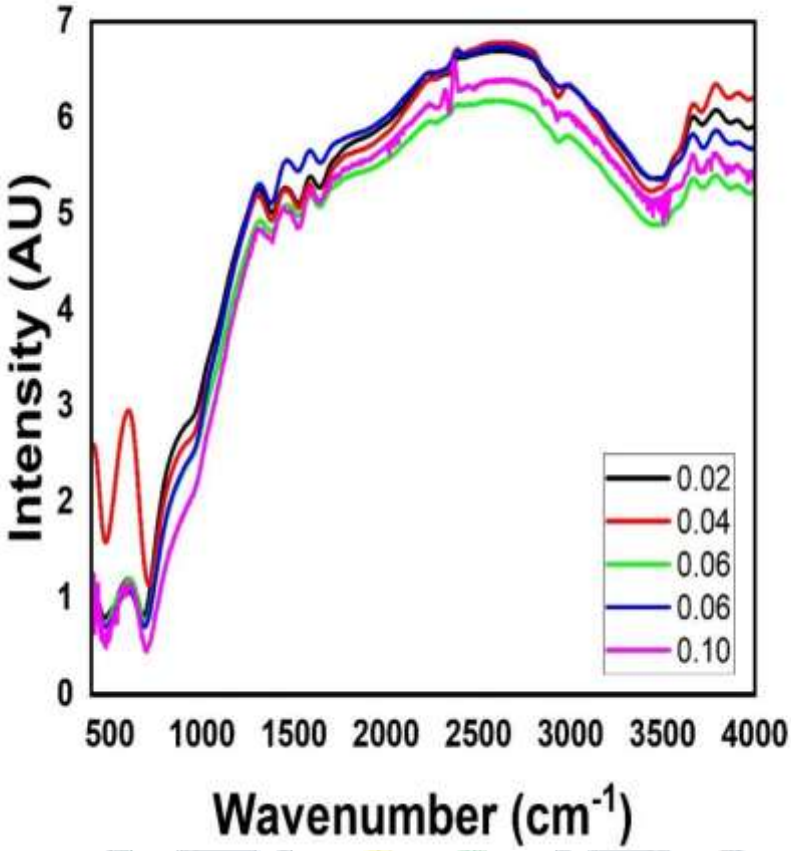

Figure (2). FTIR spectra for $Sm_xCu_{(1-x)}Fe_2O_4$ (x=0.02 to 0.10) compound.

3.3 UV-Visible Spectra Analysis

The estimation of band gap in inorganic compounds is a crucial factor as it deals with optical properties such as photocatalysis, luminescence. Fig. 3 shows UV-visible spectra for $Sm_xCu_{(1-x)}Fe_2O_4$ compounds measured between 275 – 1000 nm wavelength range. Two independent absorption peaks were observed for all Sm concentrations of the samples which are due to the octahedral and tetrahedral crystal fields of 3d orbitals of iron and copper crystals [24].

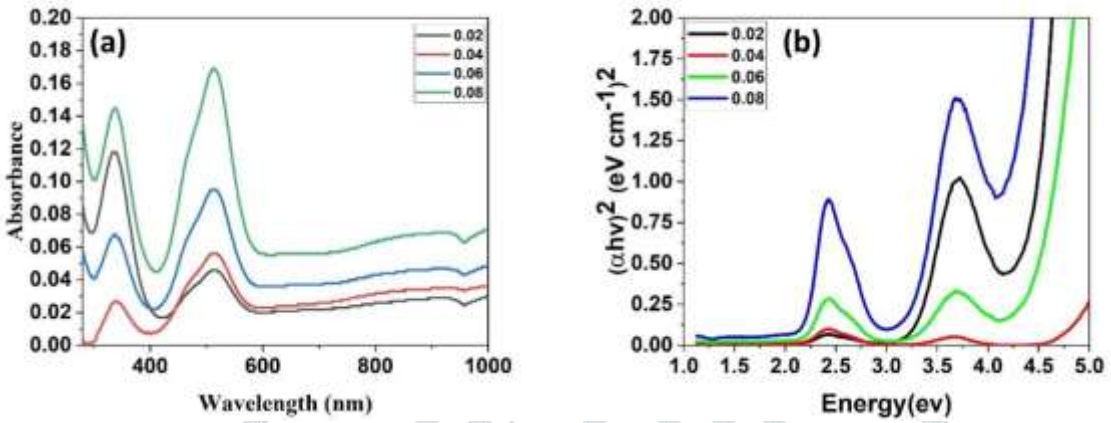

Figure (3). (a) ***UV-visible spectra*** *for* $Sm_xCu_{(1-x)}Fe_2O_4$ *(x=0.02 to 0.10) compound (b)* ***Tau-plots*** *for* $Sm_xCu_{(1-x)}Fe_2O_4$ *(x=0.02 to 0.10) compound.*

Energy band gap for these compounds are calculated from Tau's plot. The plots were obtained by considering $\alpha hv = B(hv - Eg)^{n/2}$ equation. From the equation *a, h, v, B,* and *Eg* represents coefficient of absorption, Plank's constant, frequency of light, semiconductor constant and semiconductor band-gap respectively. For n = 1, it represents allowed transition band gap is obtained [25,26]. Fig. 3 (b) respects Tau plots which were plotted between $(ahv)^2$ verses hv an example of the plot for $Sm_xCu_{(1-x)}Fe_2O_4$ (x = 0.02 to 0.10). Two band gaps were calculated which are in rage of 2.38 – 2.41 eV and 3.67 – 3.69 eV foe series of samples. It was seen that peak intensity increases with increasing Sm concentration.

From the energy band gap, refractive index for the compounds are estimated using Herve and Vandamme equation $R.I. = \sqrt{\left[1 + \left(\frac{X}{Eg+Y}\right)\right]}$ [27,28], where, X and Y are constant and their values respectively are 13.6 eV and 3.4 eV. Calculated refractive index in UV region is 2.55.

IV. Conclusions

The mentioned research work confirmed the formation of $Sm_xCu_{(1-x)}Fe_2O_4$ (x = 0.02 to 0.10) which were prepared via microwave assisted sol-gel method. XRD study suggested the compounds forms in tetragonal crystal phase with prominent peak at 36.04° and reflection plane of (211). Out of all observed plane. (211) is most dominating orientation for all $Sm_xCu_{(1-x)}Fe_2O_4$ (x = 0.02t 0.10) compounds. FTIR analysis confirmed presence of octahedral complexes of ferrite compound ions as well as tetrahedral Cu^{2+} - O^{2-} metal oxide ions. The data is consistent with the literature. Further, the UV-Visible analysis suggested presence of the 3d-orbital of Fe crystal depicting the tetrahedral and octahedral crystal field. In addition to this, calculated band gap values were in range of 2.38 – 2.41 eV and 3.67 – 3.69 eV. These energy gaps are suitable in ultraviolet and

visible region suggesting the prepared samples have photocatalytic and photovoltaic application in these regions. The refractive index also estimated as 2.54.

V. Acknowledgement

The authors express their gratitude to principal of Sardar Patel Mahavidyalaya, Chandrapur (M.S.) for providing the facilities to the research work.

References

[1]. Stojanovic, B. D., Dzunuzovic, A. S., & Ilic, N. I., 2018. "In Magnetic, ferroelectric, and multiferroic metal oxides", Elsevier, 333-359.

[2]. Alan, D., & Kay, R.,1992. "High temperature thermodynamics and applications of rare earth oxides and sulphides in ferrous metallurgy. Mineral Processing and Extractive Metullargy", Review, 10: 307-323.

[3]. Jiang, J., Goya, G., & Rechenberg, H. R.,1999. " Magnetic properties of nanostructured $CuFe_2O_4$", Journal of Physics: Condensed Matter 11: 4063.

[4]. Sun, Z., Liu, L., zeng Jia, D. & Pan, W.,2007. "Simple synthesis of $CuFe_2O_4$ nanoparticles as gas-sensing materials. Sensors and Actuators", B: Chemical 125: 144-148.

[5]. Khandekar, M. S., Tarwal, N. L., Patil, J. Y., Shaikh, F. I., Mulla, I. S. & Suryavanshi, S. S., 2013."Liquefied petroleum gas sensing performance of cerium doped copper ferrite", Ceramics International, 39: 5901-5907, doi:https://doi.org/10.1016/j.ceramint.2013.01.010.

[6]. Saadi, S., Bouguelia, A. & Trari, M.,2006. "Photo-assisted hydrogen evolution over spinel CuM_2O_4 (M=Al, Cr, Mn, Fe and Co)", Renewable Energy, 31: 2245-2256, doi:https://doi.org/10.1016/j.renene.2005.10.014.

[7]. Yang, H., Yan, J., Lu, Z., Cheng, X. & Tang, Y.,2009. "Photocatalytic activity evaluation of tetragonal $CuFe_2O_4$ nanoparticles for the H_2 evolution under visible light irradiation," Journal of Alloys and Compounds, 476: 715-719, doi:https://doi.org/10.1016/j.jallcom.2008.09.104.

[8]. Keerthana, S., Yuvakkumar, R., Ravi, G., Pavithra, S., Thambidurai, M., Dang, C. & Velauthapillai, D.,2021. "Pure and Ce-doped spinel CuFe2O4 photocatalysts for efficient rhodamine B degradation," Environmental Research, 200: 111528.

[9]. Sheena, T., Jyothish, B. & Jacob, J.,2024. "Preparation, characterization, and in vitro evaluation of the anticancer activity of Ce3+ doped $CuFe_2O_4$ spinel nanoparticles in MCF-7 cell lines," Chemical Physics Impact, **8:** 100423.

[10]. Khanh, H. B., Mittova, V. O., Nguyen, A. T. & Duyen, P. T. H.,2022. "Structural and magnetic properties of Ho-doped $CuFe_2O_4$ nanoparticles prepared by a simple co-precipitation method," Condensed Matter and Interphases, 24: 109-115.

[11]. Ergin, İ., Özçelik, S., Yalcin, B., Arda, L., İçin, K. & Özçelik, B.,2024. "Sr-doped $CuFe_2O_4$ Nanoparticles: Exploring Structural, Magnetic and Blood Compatibility Characteristics," Ceramics International.

[12]. Manikandan, V., Kuncser, V., Vasile, B., Kavita, S., Vigneselvan, S. & Mane, R., 2019. "Enhancement in magnetic and dielectric properties of the ruthenium-doped copper ferrite (Ru-$CuFe_2O_4$) nanoparticles," Journal of Magnetism and Magnetic Materials ,476: 18-23.

[13]. Dayana, P. N., Abel, M. J., Inbaraj, P. F. H., Sivaranjani, S., Thiruneelakandan, R. & prince, J. J.,2022. "Zirconium doped copper ferrite ($CuFe_2O_4$) nanoparticles for the enhancement of visible light-responsive photocatalytic degradation of rose Bengal and indigo carmine dyes," Journal of Cluster Science, 33: 1739-1749.

[14]. Nawle, A. C., Humbe, A. V., Babrekar, M., Deshmukh, S. & Jadhav, K.,2017. "Deposition, characterization, magnetic and optical properties of Zn doped $CuFe_2O_4$ thin films," Journal of Alloys and Compounds ,695: 1573-1582.

[15]. Kamel Attar Kar, M., Fazaeli, R., Manteghi, F. & Ghahari, M.,2019. "Structural, Optical, and Isothermic Studies of $CuFe_2O_4$ and Zn-Doped $CuFe_2O_4$ Nanoferrite as a Magnetic Catalyst for Photocatalytic Degradation of Direct Red 264 Under Visible Light Irradiation," Environmental Progress & Sustainable Energy, 38: 13109.

[16]. Verma, K., Kumar, A. & Varshney, D., 2013. "Effect of Zn and Mg doping on structural, dielectric and magnetic properties of tetragonal $CuFe_2O_4$," Current Applied Physics, 13: 467-473.

[17]. Zhu, Z., Li, X., Zhao, Q., Li, Y., Sun, C. & Cao, Y.,2013. "Photocatalytic performances and activities of Ag-doped $CuFe_2O_4$ nanoparticles," Materials Research Bulletin 48: 2927-2932, doi:https://doi.org/10.1016/j.materresbull.2013.04.042.

[18]. Tao, S., Gao, F., Liu, X. & Toft Sørensen, O.,2000. "Preparation and gas-sensing properties of $CuFe_2O_4$ at reduced temperature," Materials Science and Engineering: B 77: 172-176, doi:https://doi.org/10.1016/S0921-5107(00)00473-6.

[19]. Ristić, M., Hannoyer, B., Popović, S., Musić, S. & Bajraktaraj, N.,2000. "Ferritization of copper ions in the Cu–Fe–O system," Materials Science and Engineering: B **77:** 73-82, doi:https://doi.org/10.1016/S0921-5107(00)00474-8.

[20]. Wang, M., Ai, Z. & Zhang, L., 2008. "Generalized Preparation of Porous Nanocrystalline $ZnFe_2O_4$ Superstructures from Zinc Ferrioxalate Precursor and Its Superparamagnetic Property," The Journal of Physical Chemistry C, 112: 13163-13170, doi:10.1021/jp804009h.

[21]. Kong, M., Song, H., Li, F., Dai, D. & Gao, H.,2017. "Facile synthesis of $Bi_2Fe_4O_9$ nanoplate and its application as a novel adsorbent for Cu(II) removal," Journal of Environmental Chemical Engineering, 5: 69-78, doi:https://doi.org/10.1016/j.jece.2016.11.020.

[22]. Bruns, E. A., Perraud, V., Zelenyuk, A., Ezell, M. J., Johnson, S. N., Yu, Y., Imre, D., Finlayson-Pitts, B. J. & Alexander, M. L.,2010. "Comparison of FTIR and particle mass spectrometry for the measurement of particulate organic nitrates", Environmental science & technology, 44: 1056-1061.

[23]. Selvan, R. K., Augustin, C., Berchmans, L. J. & Saraswathi, R.,2003. "Combustion synthesis of $CuFe_2O_4$, " Materials Research Bulletin ,38: 41-54 .

[24]. Wang, X., Zhang, M., Tian, P., Chin, W. S. & Zhang, C. M.,2014. "A facile approach to pure-phase Bi2Fe4O9 nanoparticles sensitive to visible light," Applied Surface Science, **321:** 144-149, doi:https://doi.org/10.1016/j.apsusc.2014.09.166.

[25]. Chaware, P., Nande, A., Dhoble, S. J. & Rewatkar, K. G.,2021. "Structural, photoluminescence and Judd-Ofelt analysis of red-emitting Eu3+ doped strontium hexa-aluminate nanophosphors for lighting application," Optical Materials, 121: 111542, doi:https://doi.org/10.1016/j.optmat.2021.111542,.

[26]. Pawade, V. B. & Dhoble, S. J., 2011. "Novel blue-emitting SrMg2Al16O27:Eu2+ phosphor for solid-state lighting," Luminescence, 26: 722-727, doi:https://doi.org/10.1002/bio.1304.

[27]. Sanad, M. M. S. & Rashad, M. M., 2016. "Tuning the structural, optical, photoluminescence and dielectric properties of Eu2+-activated mixed strontium aluminate phosphors with different rare earth co-activators," Journal of Materials Science: Materials in Electronics, 27: 9034-9043, doi:10.1007/s10854-016-4936-0 .

[28]. Hervé, P. & Vandamme, L. K. J.,1994. "General relation between refractive index and energy gap in semiconductors," Infrared Physics & Technology, 35: 609-615, doi:https://doi.org/10.1016/1350-4495(94)90026-4.